

A Study on Highly Efficient Organic Electroluminescent Devices

Jae Hoon Park[**], **Yong Soo Lee**[**], **and Jong Sun Choi**[*]

Abstract

In order to improve the device performances of organic electroluminescent devices (OELDs), the efficiency of carrier injections into the organic layers from electrodes and the balance of injected carrier densities in the emission region are critical factors. Especially, energy barriers, which exist at the interfaces between electrodes and organic layers, interrupt carrier injections, which lead to unbalanced carrier densities. In this study, α-septithiophene (α-7T), as a buffer layer, and composite cathode composed of Al and CsF were formed to improve hole and electron injections, respectively. The orientations of α-7T molecules were adjusted using the simple rubbing method and the mass ratio of CsF was varied from 1 to 10 wt%. Upon investigation of we believe that the 3 wt% mass ratio of CsF and the horizontal orientation of α-7T molecules are the optimized conditions for achieving better the performance of OELDs. Device with the horizontally oriented 20 nm thick α-7T layer and composite cathode shows a turn-on voltage of 7V and luminance of 172 cd/m^2 at 4 mA/cm^2.

Keywords : Organic electroluminescent devices, buffer layer, composite cathode, alkaline metal, α-septithiophene

1. Introduction

Since the development of organic electroluminescent devices (OELDs) [1], by Tang and Van Slyke many efforts have been made to improve device efficiency [2~4]. Device efficiency is highly dependent on carrier injecting processes at electrode and organic interfaces. Thus, the carrier recombination efficiency is an important factor affecting the emission efficiency [5]. Enhanced carrier injections and transport to the emission region do not ensure that device efficiency, will be improved but it strongly depends on the balanced carrier injections from electrodes and efficient recombinations of the carriers at the emission region [6]. Organic conducting layers, inserted between anode and organic layer, and low work function cathodes are commonly for hole and electron injections, respectively.

In this work, we demonstrate that OELD performances can be improved by enhanced and balanced carrier injections into organic layers. Thin α-7T layer was inserted as a buffer layer. CsF and Al were both evaporated simultaneously for composite cathode. Using these structures, we were able to improve device performances, which shall be discussed in the following sections.

2. Experiments

Devices were fabricated on ITO-patterned glass substrates. The ITO film had a sheet resistance of less than 20Ω/ and was about 100 nm thick. And ITO-patterned substrates were cleaned in ultrasonic baths of acetone, isopropyl alcohol, and then D. I. water, successively. Then, they were dried in nitrogen gas flow and conveyed to a vacuum oven to be heated up to 180 °C for 20 min to eliminate the residual solution. The

Manuscript received May 17, 2003; accepted for publication June 23, 2003.
This work was supported by the Korea Research Foundation (KRF-2001-005-D22001).
* Member, KIDS; ** Student Member, KIDS.
Corresponding Author : Jae Hoon Park
Department of Electrical, Information, and Control Engineering, Hongik University 72-1, Sangsu-dong, Mapo-gu, Seoul 121-791, Korea.
E-mail : ga2310401@wow1.hongik.ac.kr **Tel** : +2 320-1488
Fax : +2 320-1110

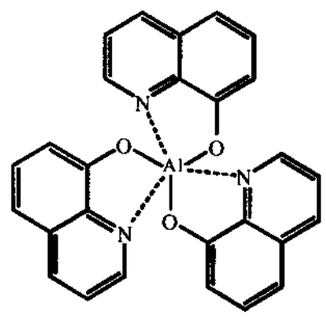

Alq_3

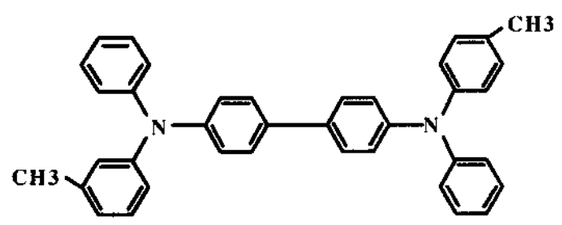

TPD

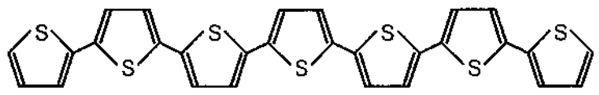

$\alpha - 7T$

(a)

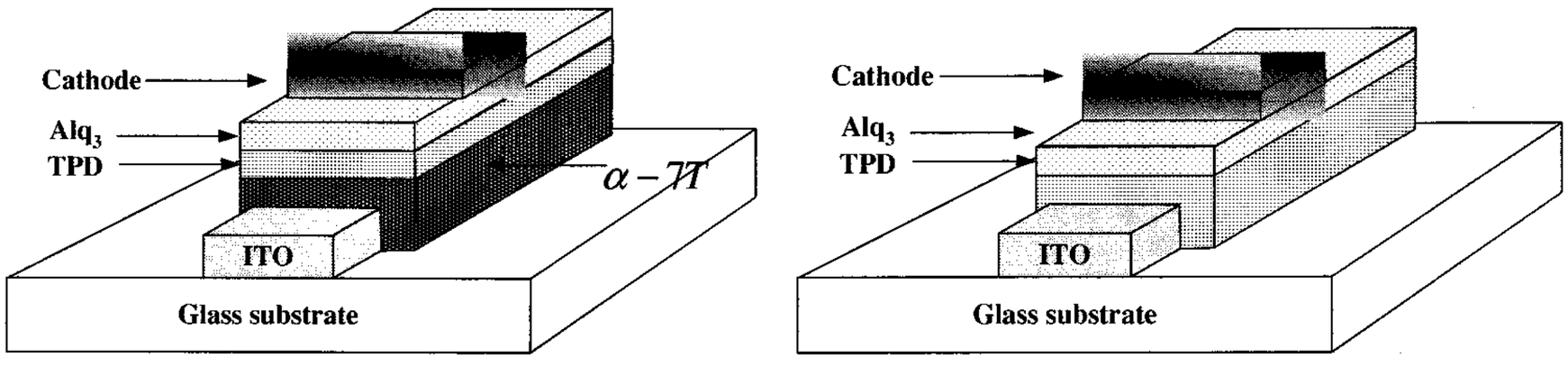

(b)

Fig. 1. (a) Molecular structures of organic materials and (b) schematics of OELDs.

molecular structures of the organic materials and the schematics of OELDs used in this study are shown in Fig. 1. Organic layers were deposited in the following sequence: an α-7T layer was deposited onto ITO as a buffer layer; and then, 50-nm-thick TPD [N, N'-diphenyl-N, N'-bis(3-methylphenyl)-1,1'-biphenyl-4-4'-diamine] and 50-nm-thick Alq_3 [tris(8-hydroxyquinoline) aluminium] were deposited as the hole- and electron-transporting layers, respectively, under a base pressure of 1.6×10^{-6} Torr. Lastly, 100-nm-thick cathode was evaporated under the same pressure.

The rubbing process for the horizontal orientation of α-7T molecules was adopted, which was described elsewhere [7,8]. In depositing the Al-CsF composite contact, the mass ratio of alkaline metal was varied from 1 to 10 wt%. The effective cell area, which is defined with the overlap region between the anode and cathode, was 0.09 cm^2. The thicknesses of the layers were confirmed using ellipsometry (Plasmos, SD-2100) and α-step profilemeter (Tenkor, 200). UV/vis absorption was measured by using a HP 8452A unit. The diffusion depth of Cs ions was confirmed using auger electron spectroscopy (AES, PHI-670) and the surface morphology of TPD layer was observed using atomic force microscopy (AFM, Park Scientific Instrument). The current-voltage measurements were performed using Keithley 238 source-measurement unit. All measurements were carried out at room temperature and under an ambient atmosphere.

3. Results and Discussion

The absorption spectra of α-7T layers with different molecular orientations under polarized lights are shown in Fig. 2. The rubbing method was used for the horizontal molecular orientation to the substrate, In the absorption spectra of α-7T film (50 nm) with rubbing-induced molecular orientation, the absorption was strong when the light was parallel to the rubbing direction, whereas the absorption became very weak when the light was perpendicular to the rubbing direction. The dichroic ratio, $R=A_{//}/A_{\perp}$, was 4.2 at 438 nm, where $A_{//}$ and $A_{\perp}$ were the absorbances of α-7T films whose molecules were parallel and perpendicular to the substrate,

respectively. The spectra present a broad-band peak at 438 nm with the satellites at 488 and 534 nm, which represents the fundamental π-π* transition of the isolated molecule and its vibronic replicas [7]. The fundamental π-π* band peak at 438 nm became highly dichroic. Meanwhile, dichroism was not observed in the absorption spectra for an un-rubbed α-7T layer. Only a broad-band peak at 380 nm was observed. These results prove that the orientations of the rubbed α-7T molecules are parallel to each other and horizontal to the substrate.

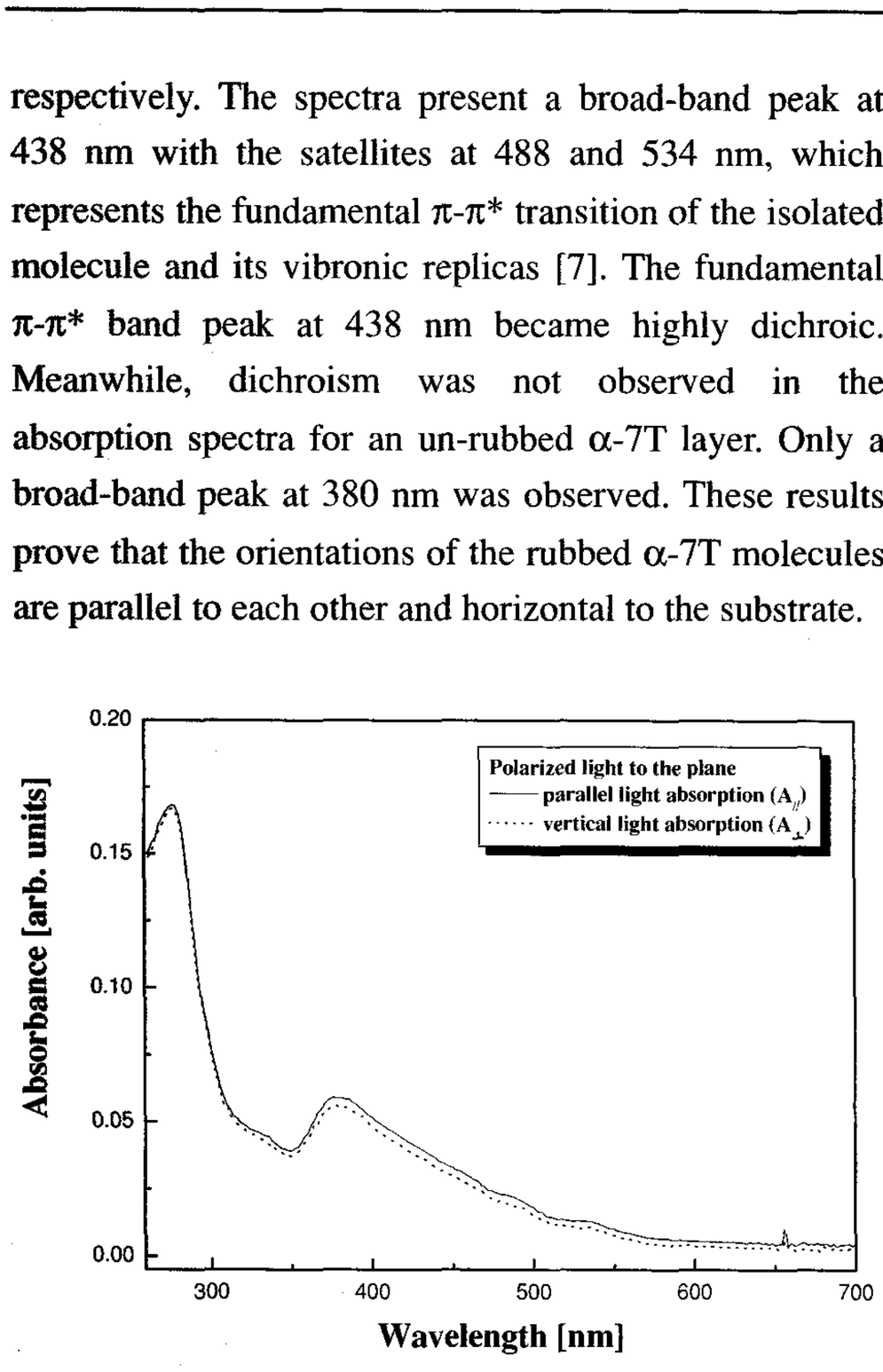

(a)

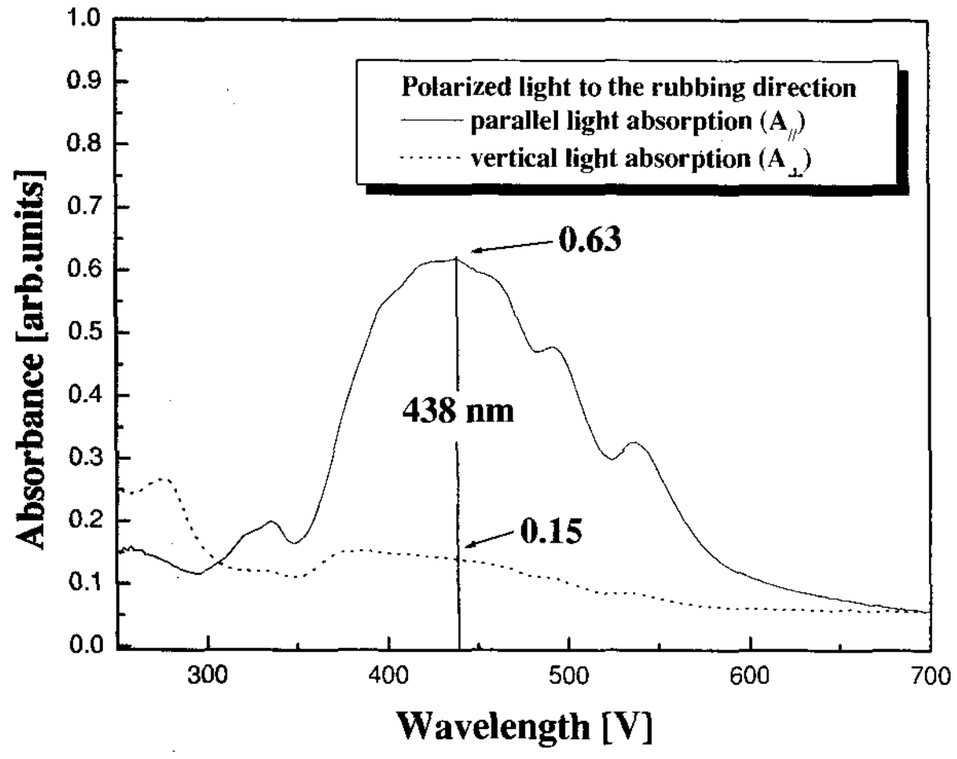

(b)

Fig. 2. UV/vis spectra of (a) the un-rubbed α-7T layer and (b) the rubbed α-7T layer.

AFM was used to investigate the initial growth mode of TPD layer on α-7T layer. The sample formed from α-7T/TPD layer showsed a very flat and smooth interface with the rms roughness of about 12 Å, because α-7T layer prevents TPD layer from directly contacting with the bare ITO, as shown in Fig. 3. Therefore, it is believe that the insertion of α-7T layer can reduce the bias stress of TPD layer during the device operation, which and leads to the stable operation.

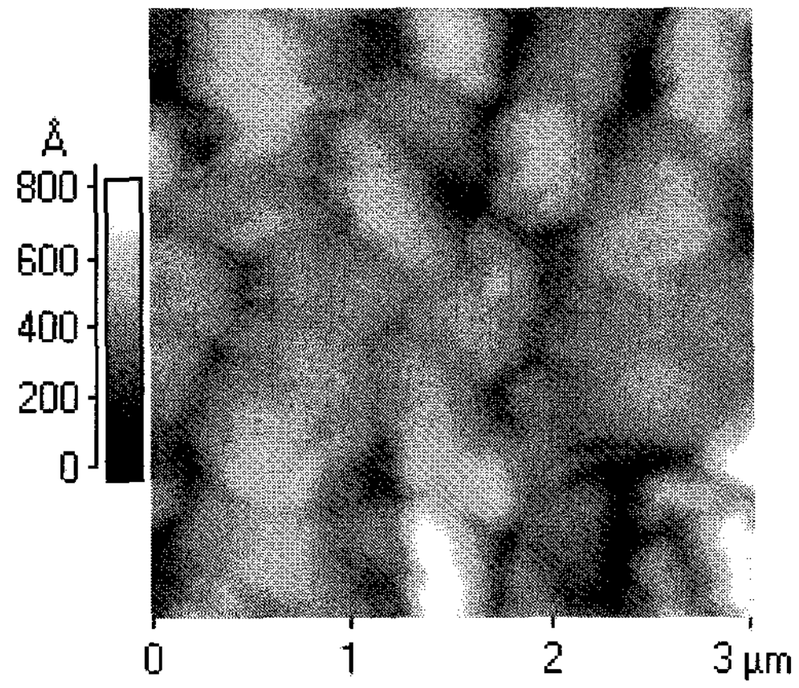

(a)

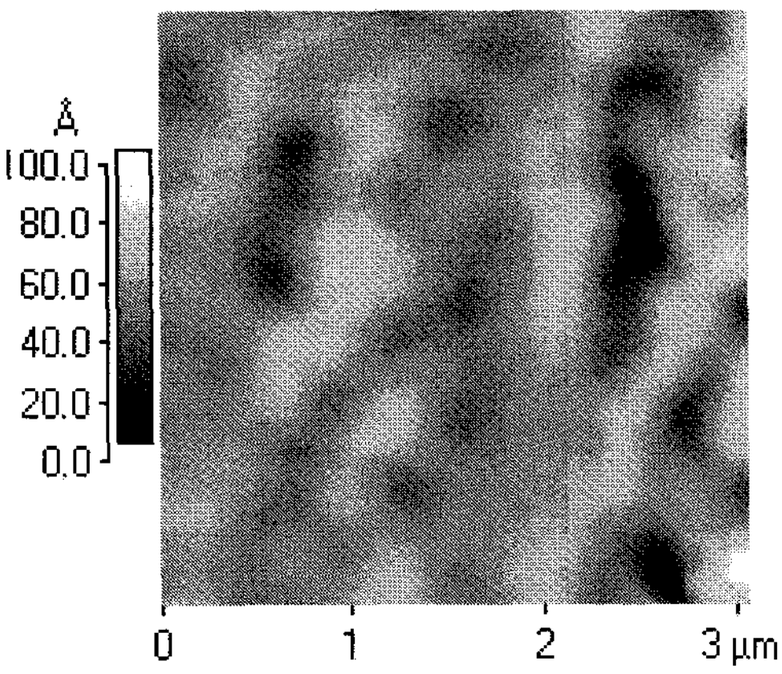

(b)

Fig. 3. AFM images of TPD layer. (a) TPD on the bare ITO (rms roughness, 102 Å) and (b) TPD on the rubbed α-7T layer (rms roughness, 12 Å).

The current density-voltage characteristics for various thicknesses and orientations of α-7T layer are shown in Fig. 4. The device with the horizontally oriented 20 nm thick α-7T layer shows superior characteristics over others. This result is assumed to be attributed to enhanced hole-transport along the highest occupied molecular orbital (HOMO) column running through the horizontal film [9]. The inclusion of buffer layers has only a modest effect on the efficiency as long as these layers are sufficiently thin (below 20 nm) [10]. Therefore, it is believed that the horizontally oriented α-

7T layer (20 nm) can enhance the device performance.

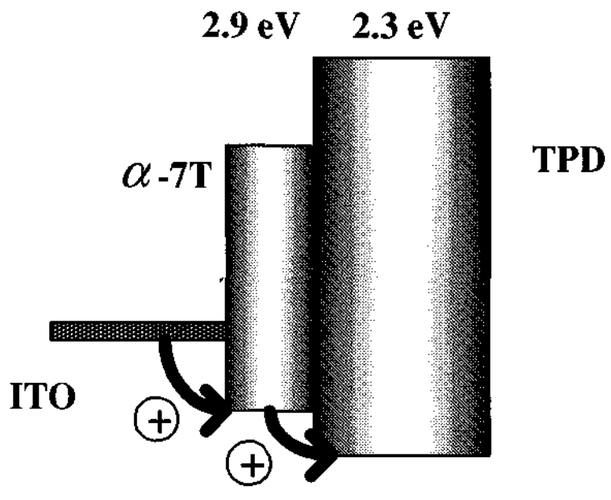

(a)

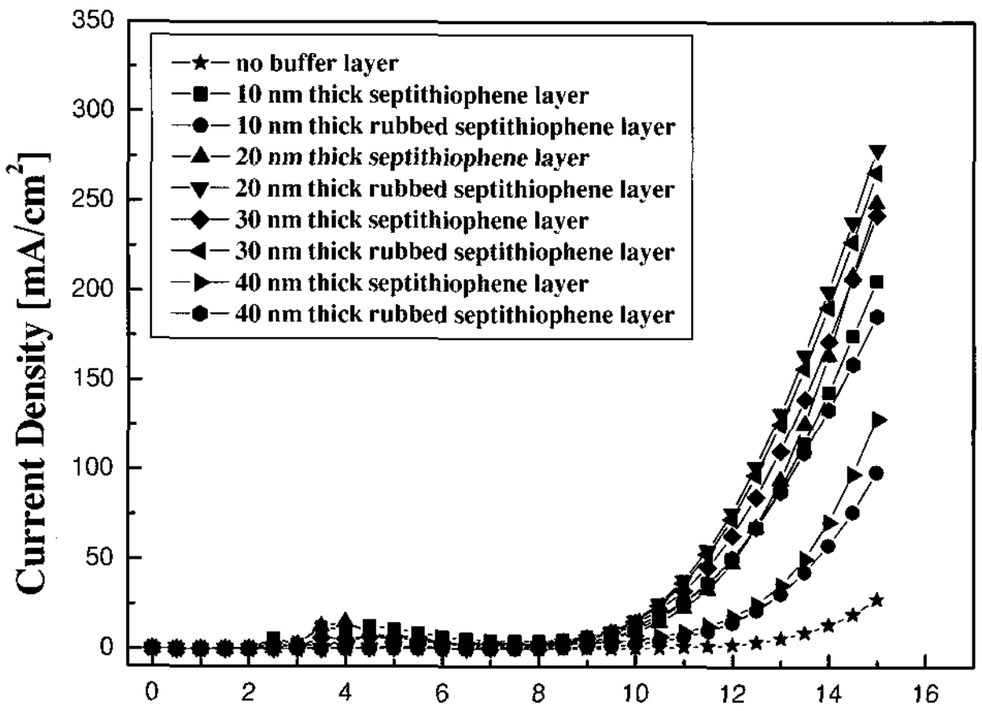

(b)

Fig. 4. (a) Hole injection process via α-7T buffer layer and (b) the current density-voltage characteristics of OELDs according to the different thicknesses of α-7T layer.

The current density-voltage characteristics of the devices with the composite cathodes are shown in Fig. 5. The mass ratio of CsF was varied from 1 to 10 wt%. The devices with the composite cathodes show superior performance to the device with Al cathode. Low operation voltages were obtained, which is attributed to the efficient electron injections. CsF molecules are decomposed when contact with Al atoms. AES spectrum shows that the diffusion depth of Cs into Alq_3 is about 25 nm, as shown in Fig. 6. The energy level of organic layer was adjusted due to the diffused cesium ions into the organic layer. The electron from fluorine was transferred back to the cesium atom and an extra charge gets transferred to the organic layer. As a result, the contact formed at the organic/cathode interface became ohmic [11]. It is reported that Cs is evaporated onto Alq_3 and diffused uniformly into Alq_3 so that the Fermi level moves toward the lowest unoccupied molecular orbital (LUMO) level of Alq_3 [12]. Therefore, efficient electron injections can be achieved by lowered energy barrier. It is considered that the cathode composed of Al-CsF (3 wt%) is suitable for improving the device performances.

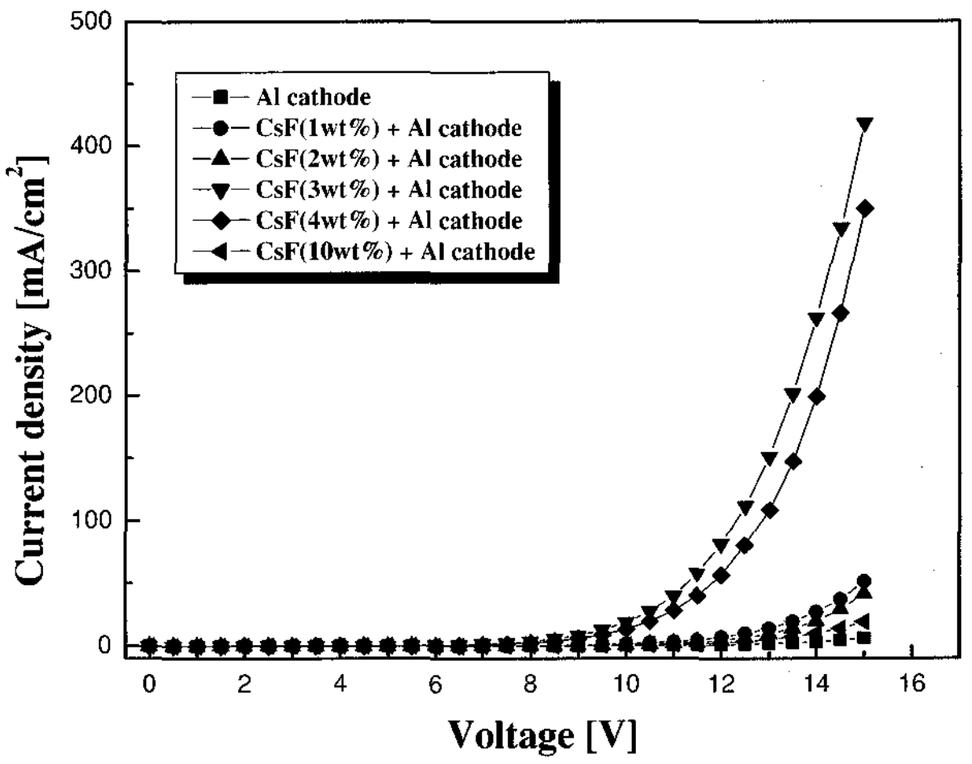

Fig. 5. The current density-voltage characteristics of OELDs with composite cathode according to the mass ratios of alkaline metal.

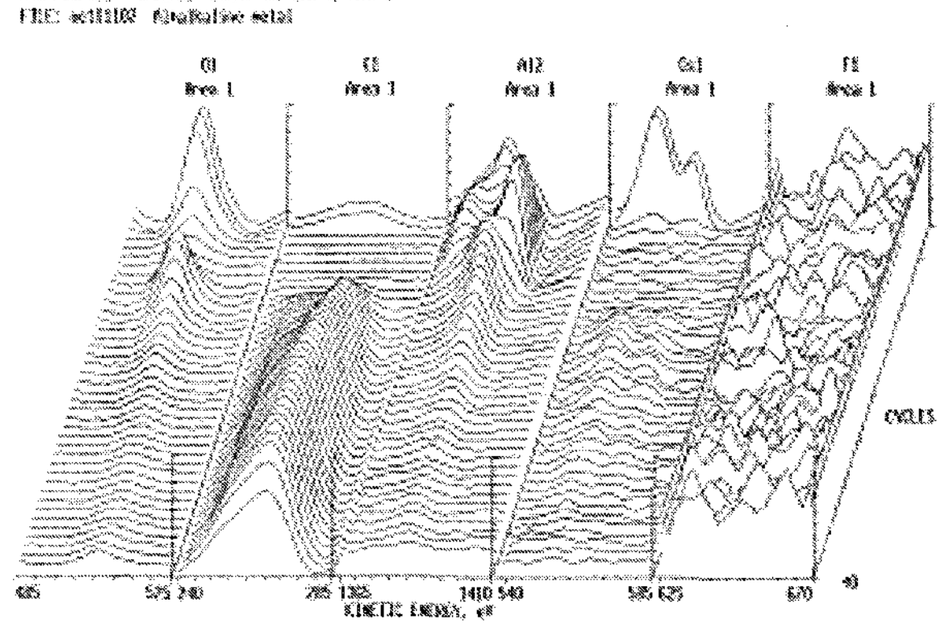

Fig. 6. AES characteristic of composite cathode.

In order to balance the hole and electron densities in the emission region, a device with the horizontally oriented α-7T layer and composite cathode was fabricated and compared with the other devices. The current density-voltage and the luminance-voltage characteristics of the fabricated devices are show in Fig. 7. Device with the rubbed α-7T layer and composite cathode showed the largest current density at the same voltage and the lowest turn-on voltage, 7 V. The turn-on

voltages, which are defined as a voltage at 1 cd/m^2 in this experiment, are summarized in Table 1. It also shows the highest luminance, 172 cd/m^2 at 4 mA/cm^2. Luminance characteristics at 4 mA/cm^2 are described in Table 2. These results are due to the improved carrier injections from both electrodes and the balanced carrier densities.

Table 1. Turn-on Voltage of the Fabricated Devices

Device	Turn-on Voltage
Device with Al cathode and without buffer layer	10 V
Device with the horizontally oriented α-7T layer	9 V
Device with composite cathode	9 V
Device with the horizontally oriented α-7T layer and composite cathode	7 V

Table 2. Luminance Characteristics of the Fabricated Devices

Device	Luminance at 4mA/cm^2
Device with Al cathode and without buffer layer	95 cd/m^2
Device with the horizontally oriented α-7T layer	110 cd/m^2
Device with composite cathode	160 cd/m^2
Device with the horizontally oriented α-7T layer and composite cathode	172 cd/m^2

4. Conclusions

We fabricated devices with α-7T buffer layer and Al-CsF composite cathode. Upon the investigations, the horizontally oriented α-7 with 20 nm and the composite cathode composed of Al-CsF (3 wt%) were found to be the optimized conditions for hole and electron injections, respectively. Especially, the diffusion depth of Cs ion was revealed to be about 25 nm by AES. In the device with this structure, carrier injections could be improved by lowering the energy barriers for carrier injections at electrode/organic interfaces. Device with this structure shows the lowest turn-on voltage, 7 V and the highest luminance characteristics, 172 cd/m^2 at 4 mA/cm^2. Thus, it can be concluded that the balanced carrier injections in the emission region by enhanced carrier injections into organic layers is a promising method for improving the performances of OELDs.

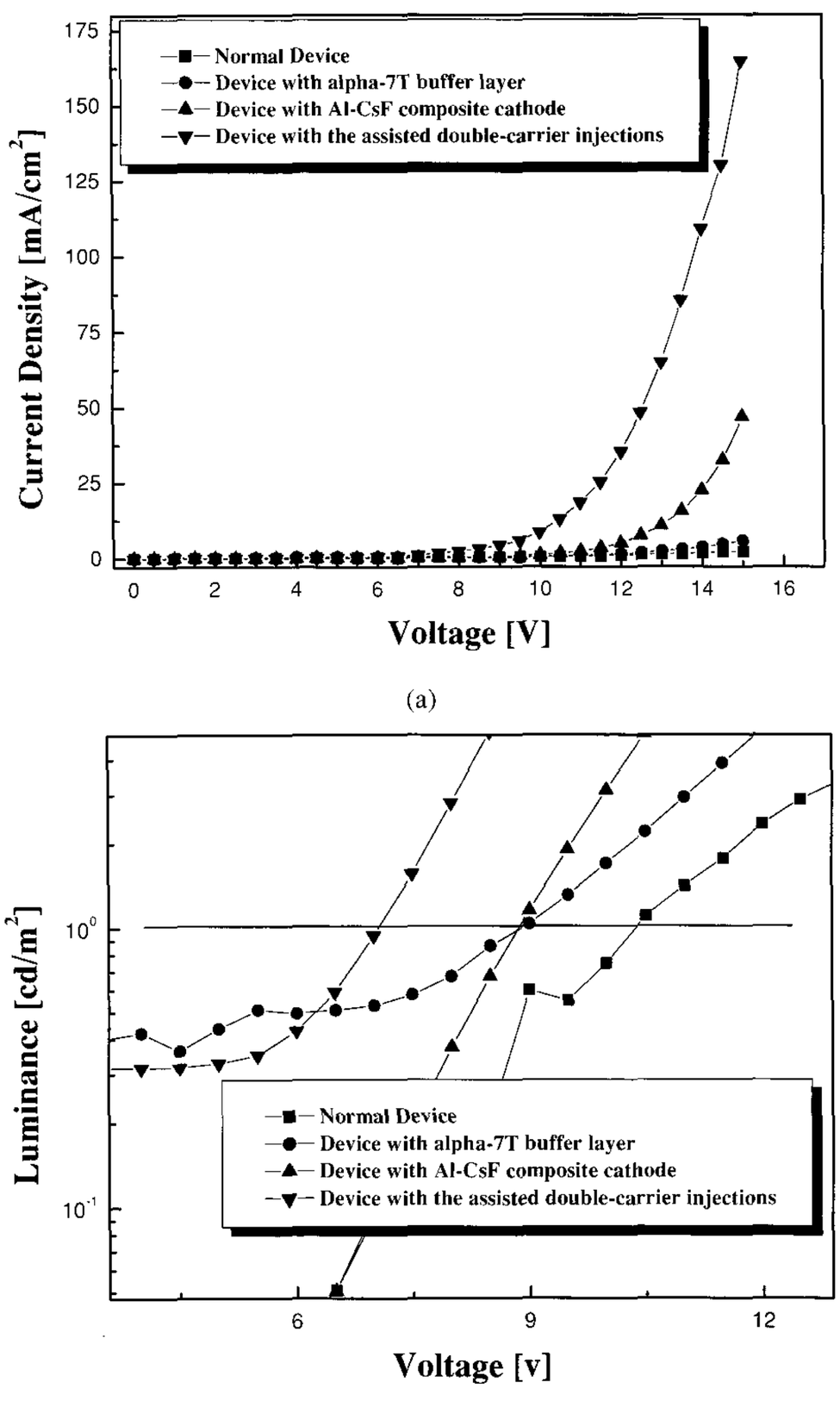

Fig. 7. (a) The current density-voltage characteristics and (b) the luminance-voltage characteristics of the fabricated devices.

References

[1] C. W. Tang and S. VanSlyke, Appl. Phys. Lett. **51**, 913 (1987).
[2] C. Hosokawa, H. Higashi, H. Nakamura, and T.

Kusumoto, Appl. Phys. Lett. **67**, 25 (1995).
[3] T. Shimada, K. Hamaguchi, and A. Koma, Appl. Phys. Lett. **72**, 15 (1998).
[4] G. Parthasarathy, P. E. Burrows, V. Khalfin, G. G. Kozlov, and S. R. Forrest, Appl. Phys. Lett. **72**, 17 (1998).
[5] D. M. Shin, S. T. Lim, J. S. Choi, and J. S. Kim, Thin Solid Films **363**, 268 (2000).
[6] J. Pommerehne, H. Vestweber, Y. H. Tak, and H. Bassler, Synth. Met. **76**, 67 (1996).
[7] C. Videlot and D. Fichou, Synth. Met. **102**, 885 (1999).
[8] J. H. Park, Y. H. Kwak, Y. S. Lee, J. S. Choi, S. T. Lim, and D. M. Shin, Mol. Cryst. Liq. Cryst., in press.
[9] H. Yanagi and S. Okamoto, Appl. Phys. Lett. **71**, 2563 (1997).
[10] J. H. Park, Y. S. Lee, Y. H. Kwak, and J. S. Choi, KIEE International Transactions on EA **11C-3**, 43 (2001).
[11] G. Parthasarathy, C. Shen, A. Kahn, and S. R. Forrest, J. Appl. Phys. **89**, 4986 (2001).
[12] G. Greczynski, W. R. Salaneck, and M. Fahlman, Appl. Surface Science **175-176**, 319 (2001).